

# Subfemtosecond pulses in the multicascade stimulated Raman scattering

A. E. Kaplan and P. L. Shkolnikov

*Department of Electrical and Computer Engineering, The Johns Hopkins University, Baltimore, Maryland 21218*

Received April 20, 1995; revised manuscript received August 13, 1995

We explore recently predicted multifrequency  $2\pi$  solitons in multicascade stimulated Raman scattering (SRS) that was mode locked by the dynamics of population at a Raman quantum transition; we show that these solitons are eigensolitons of a general solitary-wave solution. Soliton components at each frequency are bright pulses of the same (Lorentzian) shape, in contrast to the familiar bright–dark soliton pair in regular SRS and to  $1/\cosh$  regular  $2\pi$  solitons. Coherent interference of these components gives rise to a train of well-resolved subfemtosecond pulses. From an observation viewpoint the simplest SRS  $2\pi$  solitons are so-called bright–bright solitons in noncascade SRS with either two (laser + Stokes) or three (e.g., laser + Stokes + anti-Stokes) components. © 1996 Optical Society of America

## 1. INTRODUCTION

The generation of very short coherent pulses with high repetition rates and very high intensities is of great importance for various applications in both fundamental and applied physics. The shortest optical pulse length to date, 6 fs, was achieved in 1987 based on the pulse compression technique.<sup>1</sup> It was recently proposed that a Fourier synthesizer be used<sup>2</sup> to generate subfemtosecond pulses (SFP's) by the superposition of equidistant frequencies from separate lasers synchronized by nonlinear phase locking. In our most recent study<sup>3</sup> we proposed generating solitary SFP's of unipolar (subcycle) nonoscillating electromagnetic field (EM-bubbles) of up to atomic amplitude (corresponding to the intensities  $\sim 10^{15}$ – $10^{16}$  W/cm<sup>2</sup>) in gases by direct use of the so-called half-cycle pulses. The feasibility of generating SFP by higher harmonic generation (HHG) has also been discussed<sup>4–5</sup>; it is clear, however, that SFP that is due to HHG, if observed at all, would have an energy many orders of magnitude lower than that of driving radiation.

In a recent study by Kaplan<sup>6</sup> it was proposed that another approach based on multifrequency cascaded stimulated Raman scattering (CSRS) be used. The idea of using multi-CSRS is based on the fact that CSRS, which has been known, in effect, for many years,<sup>7</sup> provides tremendously broad spectra, with the multiple CSRS lines (generated by the same pump) spread from far IR (down to a few micrometers) to extreme UV and that carry a considerable power that is due to a very high conversion efficiency; up to 40% of pump energy can be converted into CSRS lines. Provided that all these CSRS components are properly phased or locked to each other, this broad-spectrum system of CSRS lines can organize itself into a train of very short (subfemtosecond and subcycle) pulses in which each of the pulses has a length (time duration) of the order of one cycle of the highest-frequency component (which can be much shorter than the cycle length of the pump radiation) and extremely high intensity. An example considered here shows the feasibility of the for-

mation of a train of  $\sim 0.2$ -fs-long,  $\sim 10^{14}$ – $10^{15}$  W/cm<sup>2</sup> intensity pulses with  $\sim 8$  fs spacing between them (see Fig. 1). The potential advantages of the proposed method compared with e.g., synchronized lasers, is that the equidistance of frequencies is sustained automatically and, compared with HHG, that the achieved efficiency of conversion from laser pump into the multi-CSRS exceeds that of HHG, which is currently  $\sim 10^{-8}$ – $10^{-7}$ , by many orders of magnitude. Besides, a proposal to modulate the polarization of the driving wave in HHG<sup>5</sup> with two lasers implies the generation of envelope HHG pulses with many cycles of a single (or few) harmonic(s) inside one envelope (with their total power being even much lower than the multiharmonic pulses of Ref. 4).

To attain SFP generation, the main problem to be solved is to line up the multiple CSRS components, i.e., to phase lock them and force them to propagate with the same group velocity to overcome a walk-off effect. The supershort pulses considered here are the result of coherent interference of all the participating CSRS components, which have to be present in the same space–time area over a sufficiently long path of their interaction. Without component locking, the walk-off effect might not allow pulse formation, as the group velocities of different CSRS components over such a large spectral stretch can be substantially different. We predicted that, in the general case of multi-CSRS,<sup>6</sup> as well as for simpler two- and three-component SRS,<sup>8</sup> this problem can be solved by the formation of multicomponent solitons, whereby all the Raman components are mode locked within a  $2\pi$  soliton, reminiscent of self-induced-transparency (SIT) solitons<sup>9</sup> and related to the quantum dynamics at the Raman transition. We demonstrate here, following Refs. 6 and 8, that Raman active materials (with the transition frequency  $\omega_0$ ) can support solitons consisting of a pump laser wave (with the frequency  $\omega_L$ ) and many Stokes and anti-Stokes components with their frequencies  $\omega_j$ :

$$\omega_j = \omega_L + j\omega_0, \quad j = \pm 1, \pm 2, \pm 3, \dots \quad (1.1)$$

One of the results of mode locking is that all these soli-

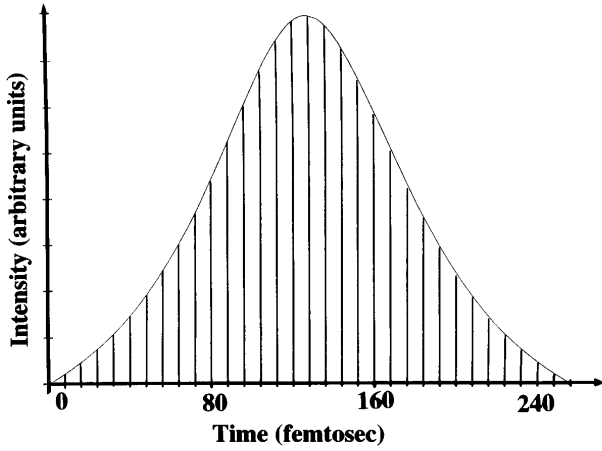


Fig. 1.  $2\pi$  SRS soliton (duration,  $\sim 100$  fs) shown by the Lorentzian envelope filled by mode-locked SFP's separated by  $\sim 8$ -fs intervals.

ton components propagate with the same group velocity (although their linear group velocities are different), have the same amplitude shape, and fully overlap in time and space. These solitons have a new, simple, Lorentzian intensity profile first found in Ref. 10 for two (laser + Stokes) components (and in Ref. 8 for three components), in contrast to well-known  $1/\cosh$  regular SIT solitons. Moreover, the coherent interference of many (instead of two or three) participating mode-locked frequency components gives rise to the train of SFP's (spaced by  $2\pi/\omega_0$ ) whose lengths are  $\sim 2\pi/\omega_{mx}$  (where  $\omega_{mx}$  is the highest anti-Stokes component frequency), i.e., much shorter than the pump cycle  $2\pi/\omega_L$ . This effect, in which the  $2\pi$  soliton plays a role of traveling shatter, can, to an extent, be related to mode-locked laser pulses formed by the coherent interference of many modes. In the effect studied here, however, the pulse formation occurs at a time scale of up to 5–6 orders of magnitude shorter than that of the mode-locked lasers. The difference between new solitons and the well-known bright–dark SRS solitons<sup>11</sup> is that all the frequency components of a new soliton are bright pulses; all of them propagate with the same group velocity and, in the case of eigensolitons, have the same shape.

High-order CSRS required for the proposed phenomenon was first observed experimentally<sup>7</sup> and understood<sup>7,12</sup> in the early 1960's, with a total number of components of up to  $\sim 10$ – $20$  and even higher (up to  $\sim 40$  in Ref. 13). The other required effect, all-bright SRS solitons, has never, to the best of our knowledge, been observed in experiment. The threshold nature of those solitons stipulates proper choice of group dispersion, driving intensity and frequency, and a sufficiently short driving pulse. Our recent estimates<sup>8</sup> showed that materials can be found to meet these requirements for two components, with the intensity requirements' being modest. Similarly, material and laser parameters could conceivably be found to satisfy the threshold conditions for CSRS solitons, for which a reward for the effort is substantially high.

In Section 2 we introduce general Maxwell + Bloch equations of the nonlinear CSRS propagation and discuss their general stationary- (solitary-) wave solution in

Section 3, and their fundamental eigensolitons, the so-called  $2\pi$  bright solitons and their fundamental properties, in Section 4. In Section 5 we discuss the simplest (noncascade) case of a two-component bright–bright SRS soliton (laser + Stokes), as well as a three-component soliton (laser + Stokes + anti-Stokes). In Section 6 we consider the formation of SFP's caused by coherent interference of many (up to 12) CSRS components.

## 2. GENERAL MAXWELL + BLOCH EQUATIONS

In the plane-wave approximation, the total CSRS field comprises  $M$  components:

$$M = M_S + M_A + 1, \quad (2.1)$$

where  $M_S$  ( $M_A$ ) is the number of cascade Stokes (anti-Stokes) components that are colinearly propagating along the axis  $z$  and can be written as

$$\text{Re} \left[ \sum_{j=-M_S}^{M_A} E_j(t, z) \exp(ik_j z - i\omega_j t) \right], \quad (2.2)$$

where  $E_j(t, z)$  is the envelope of the  $j$ th component,  $k_j = \omega_j n_j/c$ , and  $n_j = n(\omega_j)$  is the refractive index at  $\omega_j$ . The Raman quantum transition is described by the density matrix with nondiagonal elements  $\rho_{12} = \rho_{21}^*$  and the difference  $\Delta = \rho_{11} - \rho_{22}$  between populations of the lower (ground) level  $\rho_{11}$  and upper (excited) level  $\rho_{22}$ , where  $\rho_{11} + \rho_{22} = 1$ . Assuming  $\rho_{12}$  in the form

$$\rho_{12} = (i/2)\sigma(t, z) \exp(i\tilde{k}_0 z - i\omega_0 t), \quad (2.3)$$

where  $\tilde{k}_0 = (k_{M_A} - k_{-M_S})/(M - 1) \approx k_0 \equiv \omega_0/c$ , the Raman-coupled Maxwell equations for the envelopes  $E_j(t, z)$  are obtained, e.g., by using the procedure<sup>14</sup> as<sup>6</sup>

$$\begin{aligned} \frac{\partial E_j}{\partial z} + \frac{\partial E_j}{v_j \partial t} = & \frac{\pi N_a \omega_j}{\hbar c n_j} (r_{j-1,j} \xi_{j-1,j} \sigma E_{j-1} \\ & - r_{j,j+1}^* \xi_{j,j+1}^* \sigma^* E_{j+1}), \end{aligned} \quad (2.4)$$

where  $v_j = d\omega_j/dk_j$  is a group velocity at<sup>15</sup>  $\omega_j$ ,  $E_{-(M_S+1)} = E_{M_A+1} = 0$ ,  $N_a$  is the number density of Raman particles,  $\xi_{j-1,j} = \exp[i(\tilde{k}_0 + k_{j-1} - k_j)z]$  are phase mismatch factors, and

$$r_{j-1,j} = \sum_m \left[ \frac{(\mathbf{d}_{1m} \mathbf{e}_j)(\mathbf{d}_{m2} \mathbf{e}_{j-1})}{\omega_{m1} - \omega_j} + \frac{(\mathbf{d}_{1m} \mathbf{e}_{j-1})(\mathbf{d}_{m2} \mathbf{e}_j)}{\omega_{m1} + \omega_{j-1}} \right] \quad (2.5)$$

are nonlinear Raman coefficients.<sup>14,16</sup> Here  $\mathbf{d}_{1m}$  ( $\mathbf{d}_{m2}$ ) is a dipole moment of a transition between the lower (upper) Raman level and the  $m$ th quantum level,  $\omega_{m1}$  is the frequency of the  $m \rightarrow 1$  transition, and  $\mathbf{e}_j$  is the unit vector of polarization at  $\omega_j$ ; the summation is executed over all the quantum transitions except the Raman one. Equation (2.4) is valid when the local dispersion near each of the frequencies is much smaller than the large-scale dispersion between any two adjacent frequencies, which is usually the case in CSRS; we also neglected absorption by assuming that all the CSRS frequencies are sufficiently far from resonances. The dynamics of the polarization

$\sigma$  and population difference  $\Delta$  is governed by the Bloch equations generalized for two-photon processes:

$$\partial\sigma/\partial t = -\tilde{\Omega}_R^* \Delta, \quad (2.6a)$$

$$\partial\Delta/\partial t = \text{Re}(\sigma\tilde{\Omega}_R), \quad (2.6b)$$

where  $\tilde{\Omega}_R$  is a (in general, complex) Rabi frequency of the system; by using, e.g., a generalized two-level system approach<sup>14</sup> it is found as<sup>6</sup>

$$\tilde{\Omega}_R = \frac{2}{\hbar^2} \sum_{j=-M_S}^{M_A-1} r_{j,j+1} \xi_{j,j+1} E_j E_{j+1}^*. \quad (2.7)$$

The first integral of Eqs. (2.6) is a Rabi radius:

$$\Delta^2 + |\sigma|^2 = \text{const.} = 1 \quad (2.8)$$

(here  $\text{const.} = 1$ , as  $\rho_{11} + \rho_{22} = 1$ ). Because the new solitons are usually a few orders of magnitude shorter than the relaxation times of a typical Raman transition, the relaxation is neglected in Eqs. (2.6). Similarly, because the coherent lengths  $(\tilde{k}_0 + k_{j-1} - k_j)^{-1} (\gg k_0^{-1})$  are usually much larger than the spatial length of the soliton (which is especially true in gases or vapors), we also assume that  $\xi_{j-1,j} \approx 1$  (for  $M = 2$ , i.e., laser + first Stokes;  $\xi = 1$  is an exact relation). As is common in SRS theory, in Eqs. (2.4) and (2.6) we neglected small corrections to the group velocities  $v_j$  and the Stark shift of the Raman frequency  $\omega_0$ , which, if needed, can easily be accounted for (see, e.g., Refs. 14 and 16).

### 3. GENERAL STATIONARY-WAVE SOLUTION

Defining a stationary wave (of which solitary waves or solitons are a particular case) as a solution in which all the envelopes  $E_j$ ,  $\Delta$ , and  $\sigma$  propagate without change and with the same (unknown at this point) velocity  $\tilde{v}$ , using retarded coordinates

$$\eta = t - z/\tilde{v}, \quad \zeta = z, \quad (3.1)$$

and stipulating that

$$\partial E_j / \partial \zeta = 0, \quad (3.2)$$

we retain Eqs. (2.6) with  $\partial/\partial t$  replaced by  $d/d\eta$  and transform Eq. (2.4) into a set of ordinary nonlinear differential equations:

$$\delta_j d\mathcal{E}_j/d\eta = w_{j-1,j} \sigma \mathcal{E}_{j-1} - w_{j,j+1}^* \sigma^* \mathcal{E}_{j+1}, \quad (3.3)$$

where

$$\delta_j = 1/v_j - 1/\tilde{v} \quad (3.4)$$

are the group-velocity dispersion parameters,<sup>15</sup> normalized Raman coefficients  $w_{j-1,j}$  are

$$w_{j-1,j} = \frac{\pi r_{j-1,j} N_a}{c\hbar} \left( \frac{\omega_{j-1}\omega_j}{n_{j-1}n_j} \right)^{1/2}, \quad (3.5)$$

and

$$\mathcal{E}_j \equiv E_j(n_j c / 2\hbar\omega_j)^{1/2} \quad (3.6)$$

are flux amplitudes (such that  $\Phi_j = |\mathcal{E}_j|^2$  are photon fluxes of the respective components). Equations (2.6) and (3.3) yield two more integrals:

$$\sum_{j=-M_S}^{M_A} \delta_j \Phi_j = \text{const.} = I, \quad (3.7a)$$

$$2 \sum_{j=-M_S}^{M_A} j \delta_j \Phi_j(\eta) - \pi N_a \Delta(\eta) = \text{const.} = J, \quad (3.7b)$$

where Eq. (3.7a) is a Manley–Rowe-like integral. Amazingly, the set of  $M + 2$  nonlinear equations, Eqs. (2.6) and (3.3), can be solved analytically for arbitrary boundary conditions. First, using Eq. (3.3) for evaluating  $d(\mathcal{E}_j^* \mathcal{E}_{j+1})/d\eta$  and thus  $d\tilde{\Omega}_R/d\eta$  from Eq. (2.7), we find out, by using Eqs. (2.6) and (2.7), that  $d(\sigma\tilde{\Omega}_R)/d\eta$  and thus  $\sigma\tilde{\Omega}_R$  are real functions. Then, multiplying Eq. (2.6a) by  $\sigma^*$ , we find that the phase of  $\sigma$  is invariant, i.e., if  $\sigma = \rho_0 \exp(i\phi_\sigma)$  (where  $\rho_\sigma$  and  $\phi_\sigma$  are real),  $\phi_\sigma = \text{const.}$  [Applying this again to Eq. (3.3), starting from  $j = -M_S$ , one can see that all the cascade components of the stationary wave are phase locked to each other.] Without loss of generality, we can assume now that  $\phi_\sigma = 0$ , i.e., that both  $\sigma$  and  $\Omega_R$  are real functions. Using Eqs. (2.6) and (2.8), we can then express  $\Delta$  and  $\sigma$  as

$$\Delta = \pm \cos \phi_R, \quad \sigma = \sin \phi_R, \quad (3.8a)$$

where

$$\phi_R \equiv \int \Omega_R(\eta) d\eta \quad (3.8b)$$

is a Rabi phase, and the upper sign in Eqs. (3.8a) corresponds to the atoms being initially ( $\eta \rightarrow -\infty$ ) at the equilibrium  $\Delta(-\infty) = 1$ , whereas the lower sign corresponds to the an inverse population  $\Delta(-\infty) = -1$  at  $\eta \rightarrow -\infty$ . Introducing<sup>6</sup>

$$\psi \equiv \int \sigma d\eta, \quad (3.9)$$

we reduce Eq. (3.3) to the set of  $M$  linear differential equations for the envelopes  $\mathcal{E}_j$  by writing it as

$$\delta_j d\mathcal{E}_j/d\psi = w_{j-1,j} \mathcal{E}_{j-1} - w_{j,j+1}^* \mathcal{E}_{j+1}. \quad (3.10)$$

Once the eigenvalues  $\gamma_k$  of this set are evaluated, its solution is immediately found as

$$\mathcal{E}_j(\psi) = \sum_{k=1}^M c_{jk} \exp(\gamma_k \psi), \quad c_{jk} = \text{const.} \quad (3.11)$$

(Out of all the  $M^2$  constants  $c_{jk}$  in Eq. (3.11), only  $M$  are truly independent.) For the odd  $M$ 's ( $M \geq 3$ ) one of the eigenvalues is  $\gamma = 0$ .<sup>17</sup>

In the general case, the equation for nonzero eigenvalues of Eq. (3.10) have the form of a polynomial in  $\gamma^2$ . Its solution, in the simplest case of only two components<sup>8,10</sup>  $M = 2$  (i.e., laser + Stokes) is

$$\gamma^2 = -|w_{S,L}|^2/\delta_S\delta_L. \tag{3.12}$$

In the case of  $M = 3$  (e.g., Stokes + Laser + anti-Stokes, or two Stokes + laser, etc.), it is<sup>8</sup>

$$\gamma^2 = -( |w_{S,L}|^2/\delta_S\delta_L + |w_{L,A}|^2/\delta_L\delta_A ), \tag{3.13}$$

whereas, in the cases of  $M = 4$  and  $M = 5$ , it is found as<sup>6</sup>

$$\gamma^2 = -[B_1 \pm (B_1^2 - B_2)^{1/2}], \tag{3.14}$$

where

$$B_1 = \sum_j b_{j,j+1}, \quad b_{j,k} \equiv |w_{j,k}|^2/\delta_j\delta_k, \tag{3.15}$$

and for  $M = 4$  one has

$$B_2 = b_{-M_S,-M_S+1}b_{M_A-1,M_A}, \tag{3.16}$$

whereas for  $M = 5$  one has

$$B_2 = b_{-M_S,-M_S+1}b_{M_A-2,M_A-1} + b_{-M_S,-M_S+1}b_{M_A-1,M_A} + b_{-M_S+1,-M_S+2}b_{M_A-1,M_A}. \tag{3.17}$$

Using the Maxwell-equations solution [Eq. (3.11)] and noting that the Rabi frequency,

$$\Omega_R = (4/\pi N_a) \sum w_{j,j+1} \mathcal{E}_j \mathcal{E}_{j+1}^*, \tag{3.18}$$

can now be expressed as

$$\Omega_R(\psi) = \sum_{m,k=1}^M Q_{mk} \exp[(\gamma_m + \gamma_k^*)\psi], \tag{3.19}$$

where

$$Q_{mk} = Q_{mk}^* = \frac{4}{\pi N_a} \sum_{j=1}^M w_{j,j+1} c_{jk} c_{j+1,m}^*, \tag{3.20}$$

we reduce the Bloch equations [Eqs. (2.6)] to the equation,

$$d^2\psi/d\eta^2 + [1 - (d\psi/d\eta)^2]^{1/2}\Omega_R(\psi) = 0, \quad \psi \equiv \int \sigma d\eta, \tag{3.21}$$

whose general solution is readily found in quadrature form<sup>4</sup>:

$$\int \frac{d\psi}{\left\{ 1 - \left[ \int \Omega_R(\psi) d\psi \right]^2 \right\}^{1/2}} = \eta. \tag{3.22}$$

Once Eq. (3.22) is solved for  $\psi(\eta)$ , one readily obtains the dynamics of the rest of the system characteristics:  $\sigma = d\psi/d\eta$ ,  $\Delta = (1 - \sigma^2)^{1/2}$ , and, through Eq. (3.11), all the envelopes  $\mathcal{E}_j$ . In general, Eq. (3.22) gives rise to a rich family of solutions: solitary waves, stationary traveling fronts, bright and dark solitons, periodic stationary waves, etc. The solutions attributed to more than one eigenvalue  $\gamma$  may be regarded as higher-order solitons. The simplest and most fundamental are eigensolitons, i.e., those attributed to a single eigenvalue  $\gamma$ . (For  $M = 2$  and  $M = 3$  they are the only ones that are feasible as all-bright solitons.<sup>8,10</sup>

### 4. 2π BRIGHT (EIGEN)SOLITONS

For an eigensoliton, all but one coefficient  $c_{jk}$  in Eq. (3.11) vanish, such that  $\mathcal{E}_j = \bar{c}_j \exp(\gamma\psi)$ . Thus all the components of the eigenwave have the same time dependence. Of special interest is a bright soliton, i.e., a solitary eigenwave whose CSRS-components vanish at the edges:

$$\mathcal{E}_j(\eta) \rightarrow 0 \quad \text{as} \quad |\eta| \rightarrow \infty. \tag{4.1}$$

All these components have the same temporal profile,  $|\mathcal{E}_j|^2 \propto S(\eta)$ , found from Eq. (3.22) as

$$S(\eta) = \frac{\sin^2 \phi(\infty)}{2} \left\{ \cosh \left[ \frac{2(\eta - \eta_0) \sin \phi(\infty)}{\tau} \right] - \cos \phi(\infty) \right\}^{-1}, \tag{4.2}$$

where the Rabi frequency is

$$\Omega_R = 4S(\eta)/\tau, \tag{4.3}$$

$\eta_0$  is a position of the peak of the soliton {with  $S_{pk} = \cos^2[\phi(\infty)/2]$ } that can be assumed here as  $\eta_0 = 0$ ,  $\phi(\infty)$  is the initial phase of Rabi oscillations, and

$$\tau \equiv 1/\text{Re}(\gamma) \tag{4.4}$$

is the soliton length. The area of the eigensoliton is

$$\Delta\phi_R \equiv \phi_R(\infty) - \phi_R(-\infty) = 2[\pi - \phi(\infty)], \tag{4.5}$$

i.e., not necessarily an integer of  $\pi$ , a situation unusual for SIT-like solitons. In the limiting case in which  $\phi_R = \pi/2$  (i.e.,  $\Delta\phi_R = \pi$ , which corresponds to a  $\pi$  soliton), the eigensoliton has a seemingly familiar profile:

$$S(\eta) = 1/[2 \cosh(2\eta/\tau)]. \tag{4.6}$$

(Note, though, that this is an intensity profile, not the amplitude profile as in SIT solitons.) However, this soliton is due to the most unlikely initial conditions:  $\Delta(-\infty) = 0$  and  $\sigma(-\infty) = -1$ , i.e., they originate from the state in which the population is fully saturated and there are nonzero nondiagonal elements. For the intermediate solitons with  $0 < \phi(\infty) < \pi/2$ , the initial state of the system is  $\Delta(-\infty) = \pm \cos \phi(\infty)$  and  $\sigma(-\infty) = -\sin \phi(\infty) \neq 0$ . Although preparing initial states with  $\sigma \neq 0$  may not be an easy experimental task, they are still feasible (even if the finite relaxation is taken into consideration) if another short pulse is used as a precursor. Fortunately, however, a regular initial state of the system [i.e.,  $\Delta(-\infty) = \pm 1$ ,  $\sigma(-\infty) = 0$ ] can also give rise to the eigensoliton with  $\phi(\infty) = 0$ , i.e., a  $2\pi$  soliton ( $\Delta\phi_R = 2\pi$ ); it has a very simple Lorentzian profile:

$$S(\eta) = (1 + 4\eta^2/\tau^2)^{-1}, \quad \sigma = 4(\eta/\tau)S(\eta); \tag{4.7a}$$

$$\Delta = \pm[1 - 2S(\eta)], \tag{4.7b}$$

which again is unusual for SIT solitons. (For  $M = 2$ , this soliton was found in Ref. 7, and for  $M = 3$ , this soliton was found in Ref. 8.) Under the condition of Eq. (4.1)

in Eq. (3.7a),  $I = 0$ , whereas, in Eq. (3.7b),  $J = -\pi N_a$  if initially the two-level Raman system is at equilibrium [ $\Delta(-\infty) = 1$ , i.e., the upper sign in Eqs. (3.8a)]. In contrast,  $J = \pi N_a$  if the population difference was initially inverted [i.e.,  $\Delta(-\infty) = -1$ , the lower sign in Eqs. (3.8a)].

Each eigensoliton has a unique set (or eigenvector) of  $M$  components that is characterized by photon-distribution eigencoefficients,

$$\alpha_j = \text{const.}, \quad \sum |\alpha_j|^2 = 1, \quad (4.8)$$

i.e.,

$$\mathcal{E}_j(\eta) = \alpha_j \sqrt{\Phi_\Sigma} \quad \text{or} \quad \Phi_j = |\alpha_j|^2 \Phi_\Sigma, \quad (4.9)$$

where

$$\Phi_\Sigma \equiv \sum \Phi_j = \Phi_{\text{pk}} \mathcal{S}(\eta), \quad (4.10)$$

where  $\Phi_{\text{pk}}$  is a peak total photon flux. With Eq. (3.3),  $|\alpha_j|^2$  is evaluated as

$$|\alpha_j|^2 = |\beta_j|^2 \left( \sum_{j=-M_S}^{M_A} |\beta_n|^2 \right)^{-1}, \quad (4.11)$$

where  $\beta_{-M_S-1} = 0$ ,  $\beta_{-M_S} = 1$ , and for  $M_A \geq j > -M_S$ ,  $\beta_j$  can be found either through the recursion formula,

$$\beta_{j+1} = (w_{j-1} \beta_{j-1} - \gamma \beta_j \delta_j) / w_{j,j+1}^*, \quad (4.12)$$

or directly as

$$\beta_{j+1} = D_j \left( \prod_{n=-M_S}^j a_{n,n+1}^* \right)^{-1}, \quad (4.13)$$

where  $D_j$  is the determinant of a matrix whose elements  $a_{m,n}$  are defined for  $m, n \leq j$  as

$$a_{j,j} = \delta_j \gamma, \quad a_{j-1,j} = -a_{j-1,j}^* = w_{j-1,j}, \quad (4.14)$$

and  $a_{j,k} = 0$  otherwise. With Eq. (3.21),  $\Phi_{\text{pk}}$  is obtained as

$$\Phi_{\text{pk}} = \mp \pi N_a / \sum_{j=-M_S}^{M_A} j \delta_j |\alpha_j|^2, \quad (4.15)$$

where the signs correspond to those in Eqs. (3.8a). The total number of photons in the soliton is

$$P_\Sigma = \int_{-\infty}^{\infty} \Phi_\Sigma d\eta = \pi \Phi_{\text{pk}} / 2 \text{Re}(\gamma) = \pi \tau \Phi_{\text{pk}} / 2. \quad (4.16)$$

If  $P_\Sigma$  or  $\tau$  is given, one can find the velocity of the soliton,  $\tilde{v}$ . The conditions  $\text{Re}(\gamma^2) > 0$  and  $\Phi_{\text{pk}} > 0$  impose limitations on the dispersion and the nonlinearity of the system. For  $M = 2$  and  $M = 3$ , these limitations and dispersion conditions are discussed in Section 5.

## 5. TWO- AND THREE-COMPONENT BRIGHT-BRIGHT STIMULATED RAMAN SCATTERING SOLITONS

It is well known<sup>11,18</sup> that ordinary SRS (i.e., laser + Stokes) may result in the formation of peculiar solitons

that combine a so-called bright (regular) soliton at the pump (laser) frequency and a so-called dark soliton (a deep minimum in the intensity profile) at the Stokes frequency. Following experimental observations, most of the theoretical work neglected the change of populations at the Raman quantum transition. As we have shown above, if the population at the Raman transition is an essential part of the pulse dynamics in a medium with nonvanishing dispersion, SRS may result in  $2\pi$  pulses that consist, in the case of only two components, of two bright solitons at the pump and the Stokes components, both of which have a Lorentzian envelope. Theoretically discovered for  $M = 2$  a long time ago,<sup>10</sup> these solitons have not been observed experimentally, which may be attributed to their threshold nature that imposes limitations on the pulse frequency and the length for the most of the materials traditionally used for SRS. In this section we use the general theory developed above to find conditions for experimental excitation of the two- and the three-component bright-bright  $2\pi$  solitons.

The eigenvalue  $\gamma$  and the respective relaxation time  $\tau$  [Eq. (4.4)] are determined by Eqs. (3.12) and (3.13), respectively. Thus, for  $M = 2$  (laser + Stokes),

$$\tau \approx (-\delta_S \delta_L) / |w_{SL}| = \frac{c\hbar}{\pi r_{SL} N_a} \left( \frac{-\delta_S \delta_L}{\omega_S \omega_L} \right)^{1/2}, \quad (5.1)$$

and for  $M = 3$  (laser + Stokes + anti-Stokes or laser + Stokes + second Stokes),

$$\tau \approx \frac{c\hbar}{\pi N_a} \frac{|\delta_L| / (\omega_L)^{1/2}}{\{-[r_{SL}^2 (\omega_S / \delta_S) + r_{LA}^2 (\omega_A / \delta_A)]\}^{1/2}}. \quad (5.2)$$

In both these formulas we assumed that  $n \approx 1$ .

With Eq. (4.11), the coefficients  $|\alpha_j|^2$  are evaluated for the two-component soliton as

$$|\alpha_L|^2 = \delta_S / \delta_{SL} > 0; \quad |\alpha_S|^2 = -\delta_L / \delta_{SL} > 0, \quad (5.3)$$

where  $\delta_{SL} = 1/v_S - 1/v_L$  and  $\delta_{S(L)} = 1/v_{S(L)} - 1/\tilde{v}$ , and for the three-component soliton the coefficients  $|\alpha_j|^2$  are evaluated as

$$\begin{aligned} |\alpha_L|^2 &= \gamma_{(3)}^2 / W, & |\alpha_S|^2 &= |w_{SL}|^2 / \delta_S^2 W, \\ |\alpha_A|^2 &= |w_{LA}|^2 / \delta_A^2 W, \\ W &= |w_{SL}|^2 / \delta_S \delta_{SL} - |w_{LA}|^2 / \delta_A \delta_{LA}. \end{aligned} \quad (5.4)$$

The peak total photon flux  $\Phi_{\text{pk}}$  is obtained from Eq. (4.15) for  $M = 2$  as

$$\Phi_{\text{pk}} = \mp \pi N_a \delta_{SL} / \delta_S \delta_L, \quad (5.5)$$

where the signs correspond to those in Eq. (4.7b), and for  $M = 3$  as

$$\begin{aligned} \Phi_{\text{pk}} &= \pm \pi N_a (|w_{SL}|^2 / \delta_L \delta_{SL} - |w_{LA}|^2 / \delta_A \delta_{LA}) \\ & / (|w_{SL}|^2 / \delta_S - |w_{LA}|^2 / \delta_A). \end{aligned} \quad (5.6)$$

The total number of photons within the soliton pulse, defined by Eq. (4.16), for the two-component soliton is

$$P_\Sigma = \mp \pi N_a \delta_{SL} / (-\delta_S \delta_L)^{1/2} |w_{SL}|. \quad (5.7)$$

For the three-component soliton,  $P_\Sigma$  is similarly obtained by Eqs. (3.13) and (5.4).

All the values  $\gamma^2$ ,  $N_a$ , and  $|\alpha_j|^2$  are positive. This determines the following dispersion condition required for supporting a two-component soliton,  $M = 2$ , if initially the particles are at equilibrium:

$$\delta_{SL} > 0, \quad \delta_S > 0, \quad \delta_L < 0, \quad (5.8a)$$

i.e.,

$$v_s < \bar{v} < v_L; \quad (5.8b)$$

the inverse dispersion condition is required if the population was initially inverted. For the three-component soliton,  $M = 3$ , if the Raman states are initially at equilibrium, the dispersion conditions are either

$$\delta_S > 0, \quad \delta_L < 0, \quad |\delta_A| > \delta_S |\alpha_{L,A}|^2 / |\alpha_{S,L}|^2, \quad (5.9)$$

(in particular,  $v_s < \bar{v} < v_L$ ), or

$$\delta_A < 0, \quad \delta_L > 0, \quad |\delta_S| > -\delta_A |\alpha_{S,L}|^2 / |\alpha_{L,A}|^2, \quad (5.10)$$

(in particular,  $v_L < \bar{v} < v_A$ ).

As we mentioned above, the major characteristic of the bright-bright SRS soliton is that it is a threshold soliton; its parameters must satisfy threshold conditions,

$$\tau < \tau_{cr}, \quad \Phi_0 > \Phi_{cr}, \quad P_{\Sigma} > P_{cr}. \quad (5.11a)$$

For the two-component soliton,  $M = 2$ , the respective threshold (critical) values are<sup>8</sup>

$$\tau_{cr} = \delta_{SL} / |w_{SL}|, \quad (5.11b)$$

$$\Phi_{cr} = 4\pi N_a / \delta_{SL}, \quad (5.11c)$$

$$P_{cr} = 2\pi N_a / |w_{SL}| = c\alpha_{SL}^{-1} (n_S n_L / \omega_S \omega_L)^{1/2}. \quad (5.11d)$$

At the threshold,  $1/\bar{v} = (1/v_S + 1/v_L)/2$ . Note that both  $\Phi_{cr}$  and  $P_{cr}$  depend on only spectral parameters and not on the concentration of Raman particles, because  $\delta_{SL}$ ,  $w_{SL} \propto N_a$ .

The threshold conditions of inequalities (5.11) impose limitations on the parameters of both a medium and a driving field, in particular, on the pumping pulse length (or, more precisely, on the soliton length  $\tau$ ). Our estimates show that for the most of the typical SRS media,  $\tau_{cr}$  may be as short as a few femtoseconds. Thus the major requirement is the selection of material and laser frequency. One of the natural choices is electronic SRS in alkali metal vapors, e.g., in Cs vapor,<sup>19</sup> which has a high (up to 50%) conversion efficiency. For the lasers used in Ref. 17 ( $\lambda_L = 420\text{--}530$  nm), one can show that  $\tau_{cr} < 10$  fs, which is too short. The time  $\tau_{cr}$  and therefore  $\delta_{SL}$  can be increased by resonant enhancement. Such an enhancement, however, is impossible if initially only Cs ground level is populated. Indeed, the frequency of IR Stokes radiation is much lower than the frequency of any transition from Cs ground level. On the other hand, if laser frequency is close to the frequency of such a transition, then  $\delta_{SL} < 0$  (this can be shown by using the Sellmeier equation<sup>16</sup> for the refractive index of gases and vapors to evaluate the Cs refractive index). As a solution to this problem, we suggest tuning the pumping laser in such

a way that the Stokes radiation is resonant to a  $6p\text{--}5d$  transition and using another laser to slightly populate the  $6p$  level. In particular, with 467.17-nm pumping ( $\bar{\nu} \approx 21,406$  cm<sup>-1</sup>,  $\bar{\nu}_S \approx 2870$  cm<sup>-1</sup>) and because the  $6p_{3/2}$  population is  $\approx 5\%$  of that of the ground level, Eqs. (5.11) yield  $\tau_{cr} \sim 8$  ps and a critical area energy density of 0.02 J/cm<sup>2</sup>. The experiment<sup>19</sup> was conducted with a 1.3-ps 500- $\mu$ J dye laser focused confocally into a Cs-vapor column 30 cm long. Our estimates show that all the conditions of Eqs. (5.11) would be fulfilled if an additional 852.34-nm laser populated the Cs  $6p_{3/2}$  level; this would also provide the control of the soliton. Another interesting opportunity could be presented by optical fibers, for which, because of a larger dispersion, the limitations of Eqs. (5.11) on the soliton length could be relaxed.

## 6. SUBFEMTOSECOND PULSES IN MULTICOMPONENT CASCADED STIMULATED RAMAN SCATTERING $2\pi$ SOLITONS

Let us now consider the case of multiple-component CSRS, with  $M \gg 1$ , which is of main interest as far as SFP formation is concerned. To characterize the CSRS soliton fully with  $M \gg 1$ , in particular the spectral distribution of the Stokes and the anti-Stokes components in it, for a specific material, one has to account for a great

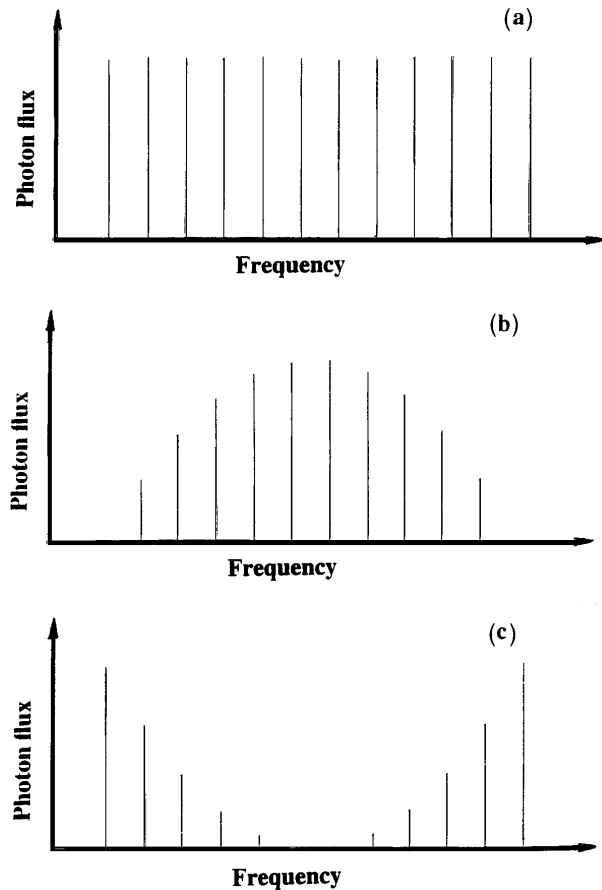


Fig. 2. Model spectral distributions used to illustrate SFP formation. The photon flux is (a) equally distributed between the components, (b) peaks in the middle of the CSRS spectrum and falls off toward both its ends (see text), (c) vanishes in the middle of the CSRS spectrum and rises up toward both its ends.

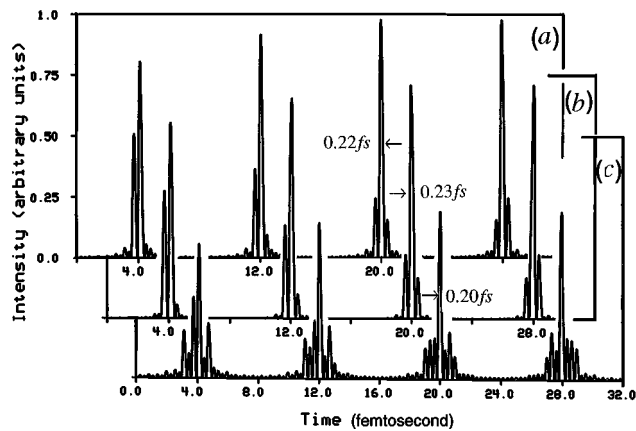


Fig. 3. SFP's (intensity versus time) in a mode-locked CSRS soliton when the photon fluxes of the CSRS components are distributed (a) as in Fig. 2(a), (b) as in Fig. 2(b), and (c) as in Fig. 2(c).

number of nonlinear spectral characteristics of the material in a very wide range of frequencies, from the far IR to the far UV. Instead, to illustrate that the SFP may appear for virtually any CSRS spectral distribution, here we choose (see Fig. 2) three substantially different model spectral distributions whereby the photon fluxes (a) are equally distributed between the CSRS components,

$$\Phi_j = \text{const.}; \quad (6.1)$$

(b) peak in the middle of the CSRS spectrum and fall off parabolically toward both its ends,

$$\Phi_j/\Phi_{\max} = 1 - 4(j - j_{\max})^2/M^2, \quad (6.2)$$

where  $j_{\max}$  is the position in the middle of the CSRS spectrum (which is usually below the driving frequency); and (c) vanish in the middle of the CSRS spectrum and rise up parabolically toward both its ends,

$$\Phi_j/\Phi_{\max} = 4(j - j_{\max})^2/M^2. \quad (6.3)$$

We choose a line with  $\lambda_0 \approx 2.4 \mu\text{m}$  (as in a H gas) pumped by the third harmonics of a Ti:sapphire laser ( $\lambda_L \approx 0.28 \mu\text{m}$ ) with 12 components. The oscillations in the time domain for all these cases are depicted in Fig. 3. In our simulation we assumed that the spacing between the pulses is much shorter than the soliton length  $\tau$  (the irregularities seen in Fig. 3 are due to incommensurability of  $\omega_L$  and  $\omega_0$ ). Distinct SFP's are evident in all the cases, and they are well separated. The length of each individual pulse is  $\sim 0.218$  fs for the distribution of Fig. 2(a),  $\sim 0.225$  fs for Fig. 2(b), and  $\sim 0.199$  fs for Fig. 2(c), although, as expected, the pulses with the most inhibited background correspond to the distribution of Fig. 2(b), and those with the least correspond to Fig. 2(c). Assuming that a significant portion of energy of the original laser pulse is trapped within a  $2\pi$  CSRS soliton, there is a good potential for attaining a high-intensity SFP by compressing the laser pulse into the SFP train. For the above example, assuming a 100-fs-long laser pulse with a cross section  $10^{-4} \text{ cm}^2$  and energy  $10^{-3} - 10^{-2} \text{ J}$ , of which  $\sim 10\%$  is trapped in a CSRS soliton of the same length, with the major part of trapped

energy concentrated in SFP, as in the case of Fig. 3(b), one obtains the peak SFP intensity of the same order as in an original laser pulse, i.e.,  $\sim 10^{14} - 10^{15} \text{ W/cm}^2$ , and even higher for better laser systems. Because in real Gaussian beams, the anti-Stokes components are usually radiated away in the far-field area as narrow cones, the SFP's should be better observed in the near-field area; however, even if only Stokes components are left in the output beam, SFP's will be broadened by only 10%–20%. Future research should address two-dimensional and three-dimensional propagation: The conical radiation of anti-Stokes components that are due to parametric processes and regular diffraction, both linear and nonlinear, under certain conditions, linear absorption (which in general is not a major factor because most of the CSRS components are far from the absorption resonances), and photoionization (which may be a significant factor for the CSRS components in the extreme UV or soft x ray<sup>20</sup>) may be considered.

In conclusion, we have demonstrated that Raman-coupled multiple CSRS components can form a  $2\pi$  soliton, with the coherent interference of the mode-locked components giving rise to the SFP train of high intensity. The first, simplest step toward their observation would be experimental observation of the simplest SRS bright–bright soliton with only two (or three) components, as in ordinary Raman scattering with laser + single Stokes (or Stokes + anti-Stokes) components.

## ACKNOWLEDGMENTS

This research is supported by the U.S. Air Force Office of Scientific Research. The authors thank B. A. Akanaev for interesting discussions.

## REFERENCES AND NOTES

1. R. L. Fork, C. H. Brito Cruz, P. C. Becker, and C. V. Shank, *Opt. Lett.* **12**, 483 (1987).
2. T. W. Hänsch, *Opt. Commun.* **80**, 71 (1990); T. Mukai, R. Wynands, and T. W. Hänsch, *Opt. Commun.* **95**, 71 (1993).
3. A. E. Kaplan and P. L. Shkolnikov, *Phys. Rev. Lett.* **75**, 2316, (1995).
4. S. M. Gladkov and N. I. Koroteev, *Usp. Fiz. Nauk* **160**, 105 (1990), *Sov. Phys. Usp.* **33**, 554 (1990); G. Farkas and C. Toth, *Phys. Lett. A* **168**, 447 (1992); S. E. Harris, J. J. Macklin and T. W. Hänsch, *Opt. Commun.* **100**, 487 (1993).
5. P. B. Corkum, N. H. Burnett, and M. Y. Ivanov, *Opt. Lett.* **19**, 1870 (1994).
6. A. E. Kaplan, *Phys. Rev. Lett.* **73**, 1243 (1994).
7. R. W. Terhune, *Solid State Design* **4**, 38 (1963); H. J. Zeiger, P. E. Tannenwald, S. Kern, and R. Burendeon, *Phys. Rev. Lett.* **11**, 419 (1963); R. Y. Chiao and B. P. Stoicheff, *Phys. Rev. Lett.* **12**, 290 (1964); P. D. Maker and R. W. Terhune, *Phys. Rev.* **137A**, 801 (1965); B. A. Akanaev, and Ya. Petselt, *JETP Lett.* **3**, 211 (1966); D. von der Linde, M. Maier, and W. Kaiser, *Phys. Rev.* **178**, 11 (1969).
8. A. E. Kaplan, P. L. Shkolnikov, and B. A. Akanaev, *Opt. Lett.* **19**, 445 (1994).
9. S. L. McCall and E. L. Hahn, *Phys. Rev. Lett.* **18**, 908 (1967).
10. T. M. Makhviladze, M. E. Sarychev, and L. A. Shelepin, *Sov. Phys. JETP* **42**, 255 (1975); T. M. Makhviladze and M. E. Sarychev, *Sov. Phys. JETP* **44**, 471 (1976).
11. K. Druhl, R. G. Wenzel, and J. L. Carlsten, *Phys. Rev. Lett.* **51**, 1171 (1983); J. C. Englund and C. M. Bowden, *Phys. Rev. Lett.* **57**, 2661 (1986), *Phys. Rev. A* **42**, 2870 (1990), *Phys. Rev. A* **46**, 578 (1992); P. C. MacPherson, R. C. Swanson, and J. L. Carlsten, *Phys. Rev. Lett.* **61**, 66 (1988), *Phys. Rev. A* **39**, 6078 (1989); C. R. Menyuk, *Phys. Rev. Lett.* **62**,

- 2937 (1989), Phys. Rev. A **47**, 2235 (1993). Bright-dark SRS solitons for more than two components (but with the dynamics of population at Raman transition neglected) were considered by J. R. Ackerhalt and P. W. Milonni, Phys. Rev. A **33**, 32 (1986) and M. Scalora, S. Singh, and C. M. Bowden, Phys. Rev. Lett. **70**, 1248 (1993).
12. R. W. Hellwarth, Phys. Rev. **130**, 1850 (1963); E. Garmire, F. Pandarese, and C. H. Townes, Phys. Rev. Lett. **11**, 160 (1963); Y. R. Shen and N. Bloembergen, Phys. Rev. **137A**, 1787 (1965).
  13. C. W. Wilkerson Jr., E. Secreta, and J. P. Reilly, Appl. Opt. **30**, 3855 (1991).
  14. V. S. Butylkin, A. E. Kaplan, Yu. G. Khronopulo, and E. I. Yakubovich, *Resonant Nonlinear Interactions of Light with Matter* (Nauka, Moscow, 1977).
  15. A nonvanishing group-velocity dispersion (even small) is essential. Without it, in the two-component case, even when the population dynamics is taken into account, the bright-bright solitons do not occur. See H. Steudel, Physica **6D**, 155 (1983). The same occurs in CSRS; see A. P. Hickman, J. A. Paisner, and W. K. Bischel, Phys. Rev. A **33**, 1788 (1986).
  16. D. C. Hanna, M. A. Yuratich, and D. Cotter, *Nonlinear Optics of Free Atoms and Molecules* (Springer-Verlag, New York, 1979), Chap. 4.
  17. These modes are continuous waves with a spectral spacing of  $2\omega_0$  (and no energy exchange between them), to an extent similar to nonlinear optical balance in nondegenerate copropagating four-wave mixing; see J. J. Wynne, Phys. Rev. Lett. **52**, 751 (1984) and in *Multiphoton Processes*, S. J. Smith and P. L. Knight, eds. (Cambridge U. Press, Cambridge, 1988), p. 318.
  18. G. P. Agrawal and R. W. Boyd, eds., *Contemporary Nonlinear Optics* (Academic, New York, 1992), pp. 72–74.
  19. R. Wyatt and D. Cotter, Opt. Commun. **37**, 421 (1981).
  20. E. Hudis, P. L. Shkolnikov, and A. E. Kaplan, Appl. Phys. Lett. **64**, 818 (1994); J. Opt. Soc. Am. B **11**, 1158 (1994); E. Hudis and A. E. Kaplan, Opt. Lett. **19**, 616 (1994).